

## Accepted Manuscript

Title: High humidity enhanced surface acoustic wave (SAW) H<sub>2</sub>S sensors based on sol–gel CuO films

Authors: Dengji Li, Xiaotao Zu, Dongyi Ao, Qingbo Tang, Yongqing Fu, Yuanjun Guo, Khan Bilawal, M. Bilal Faheem, Li Li, Sean Li, Yongliang Tang



PII: S0925-4005(19)30533-7  
DOI: <https://doi.org/10.1016/j.snb.2019.04.010>  
Reference: SNB 26379

To appear in: *Sensors and Actuators B*

Received date: 19 October 2018  
Revised date: 31 March 2019  
Accepted date: 2 April 2019

Please cite this article as: Li D, Zu X, Ao D, Tang Q, Fu Y, Guo Y, Bilawal K, Faheem MB, Li L, Li S, Tang Y, High humidity enhanced surface acoustic wave (SAW) H<sub>2</sub>S sensors based on sol–gel CuO films, *Sensors and amp; Actuators: B. Chemical* (2019), <https://doi.org/10.1016/j.snb.2019.04.010>

This is a PDF file of an unedited manuscript that has been accepted for publication. As a service to our customers we are providing this early version of the manuscript. The manuscript will undergo copyediting, typesetting, and review of the resulting proof before it is published in its final form. Please note that during the production process errors may be discovered which could affect the content, and all legal disclaimers that apply to the journal pertain.

# High humidity enhanced surface acoustic wave (SAW)

## H<sub>2</sub>S sensors based on sol–gel CuO films

*Dengji Li<sup>a</sup>, Xiaotao Zu<sup>a,\*</sup>, Dongyi Ao<sup>a</sup>, Qingbo Tang<sup>a</sup>, Yongqing Fu<sup>d</sup>, Yuanjun Guo<sup>a</sup>,*

*Khan Bilawal<sup>a</sup>, M.Bilal Faheem<sup>c</sup>, Li Li<sup>a</sup>, Sean Li<sup>e</sup>, Yongliang Tang<sup>b,\*</sup>*

<sup>a</sup> School of Physics, University of Electronic Science and Technology of China,

Chengdu, 610054, People's Republic of China

<sup>b</sup> School of Physical Science and Technology, Southwest Jiaotong University,

Chengdu, 610031, People's Republic of China

<sup>c</sup> Institute of Fundamental and Frontier Sciences, University of Electronic Science and

Technology, Chengdu 610054, P.R. China

<sup>d</sup> Faculty of Engineering and Environment, Northumbria University, Newcastle upon

Tyne, NE1 8ST, UK

<sup>e</sup> School of Materials Science & Engineering, UNSW SYDNEY, NSW 2052, Australia

\*Correspondence to: Xiaotao Zu: xtzu@uestc.edu.cn;

Yongliang Tang: tyl@swjtu.com

### Highlights

- The sensor can detect H<sub>2</sub>S gas with a concentration as low as 0.5 ppm.
- The frequency shift of sensor is derived from the change of mass loading on films.
- The responses became much faster and stronger with the increase of RH.

**Abstract**

Surface acoustic wave (SAW) sensors based on sol–gel processed porous and nanoparticulate CuO films were explored for H<sub>2</sub>S detection operated at room temperature. The SAW sensor showed a negative frequency shift when exposed to H<sub>2</sub>S gas, due to the mass loading effect on the sensitive CuO film. It has a high sensitivity of H<sub>2</sub>S, a detection limit of 500 ppb and a good selectivity to H<sub>2</sub>S gas compared with H<sub>2</sub>, C<sub>2</sub>H<sub>5</sub>OH, acetone, NH<sub>3</sub>, CO, NO, NO<sub>2</sub> gases. Relative humidity (RH) was identified to have a critical influence on the sensing performance of the sensor. The responses became much faster and stronger with the increase of RH. The significant enhancement in the sensing performance is attributed to that the chemical reaction between H<sub>2</sub>S and CuO is hindered and the physical adsorption of CuO to H<sub>2</sub>S is enhanced.

**Key words:** SAW sensors, H<sub>2</sub>S, CuO, physical adsorption, RH.

## 1. Introduction

Precision detection of hazardous gases (such as  $\text{NH}_3$ ,  $\text{NO}$ ,  $\text{NO}_2$ ,  $\text{CO}$ ,  $\text{H}_2\text{S}$ ) has become crucial in recent years due to wide applications of explosives, combustible, flammable and toxic gases in industry, military and daily activities [1-5]. Among these toxic gases, hydrogen sulfide ( $\text{H}_2\text{S}$ ), a colorless gas with foul odor like rotten eggs, is generally produced in decomposition of organic matters, human and animal's wastes, food processing, cooking stove, craft paper mills, tanneries, oil refineries and other industrial activities [6-10]. It is one of the most highly toxic gases, which can irritate eyes, skin and mucous membranes, as well as damage nervous systems of human-beings even at low concentrations [11, 12]. Therefore, the detection and monitoring of very low concentrations of  $\text{H}_2\text{S}$  in environment is highly crucial and required.

Compared to other commonly used  $\text{H}_2\text{S}$  gas sensors such as semiconductor and electrochemical sensors, surface acoustic wave (SAW) sensors have advantages of high sensitivity, good stabilization, high selectivity and low cost, as well as wireless control [13]. A typical SAW gas sensor is essentially an oscillator consisted of an amplifier and a resonator coated with a sensitive film [14, 15]. The wave energy is mainly concentrated on the surface of SAW devices within one or two wavelengths, therefore, any perturbations or changes on sensitive film, such as mass loading, conductivity, temperature and pressure, etc., will have significant impact on the propagation of waves, thus leading to frequency shift of SAW sensors. Therefore, sensitive films are the essential component of SAW sensors.

Previous studies have shown that cupric oxide (CuO) is an excellent candidate for H<sub>2</sub>S sensing [17-19]. For example, Sonia et al. fabricated a H<sub>2</sub>S semiconductor sensor based on CuO thin films, which has a response of 37.7 to 10 ppm H<sub>2</sub>S [20]. Hu al. fabricated an H<sub>2</sub>S semiconductor sensor based on Pd-doped CuO nano-flowers, which had a response of 63.8 to 1 ppm H<sub>2</sub>S [21]. Owing to its extraordinary adsorptive capability to H<sub>2</sub>S [22-24], CuO has ability to capture H<sub>2</sub>S molecules from ambient environment (e.g., through physical adsorption) and then further react with these molecules (through chemical reactions). These reactions generate CuS or Cu<sub>2</sub>S on the surface of CuO particles [25]. Both these two generated phases may change physical and chemical properties of CuO, such as its mass, elastic modulus and electrical conductivity, thus the CuO film sensing layer is suitable for SAW H<sub>2</sub>S gas sensors.

In this study, the porous CuO films are prepared using a sol-gel method for H<sub>2</sub>S gas sensing. In addition, ambient relative humidity (RH) is found to have a significant impact on the sensing performance of sensors and the mechanisms are investigated.

## 2. Experimental details

The SAW resonator was fabricated on a ST-cut ( $42^\circ 75'$ ) quartz substrate, consisted of input and output interdigital transducers (IDTs, 30 pairs each other) and 100 pairs of reflection gratings. The IDTs with a periodicity of  $16\ \mu\text{m}$  were formed using a conventional lift-off method with a sputtered 200 nm aluminum layer. The aperture of the IDTs was 3 mm.

CuO sensitive films were prepared using a sol-gel process. Following the procedure [26], copper acetate monohydrate ( $\text{Cu}(\text{CH}_3\text{COO})_2 \cdot \text{H}_2\text{O}$ ) was dissolved into 2-methoxyethanol–monoethanolamine (MEA) solutions with a concentration of 0.25 mol/L. The molar ratio of the MEA to Cu was 2:1. The resultant solutions were stirred at room temperature for half an hour to yield homogeneous sols, which were then aged for 12 hours. After that, the sols were coated onto the entire surface of the SAW resonators at a speed of 8000 rpm/min for 25s. The coated SAW resonators were immediately heated at  $250^\circ\text{C}$  for 5 min. After repeating this procedure for several times, the SAW resonators were annealed at a temperature of  $400^\circ\text{C}$  for 2 hours.

The coated SAW resonator was connected to the oscillator circuits to form a SAW sensor as shown in Fig. 1. The sensor was mounted inside a testing chamber with a volume of 20 L in an ambient environment at room temperature. The concentration of  $\text{H}_2\text{S}$  in the chamber was controlled by injecting diluted  $\text{H}_2\text{S}$  gas with different concentrations through a high-precision syringe. The frequency shift, which indicated the responses of sensors, was measured using a frequency counter (Agilent 53210A). Electrical measurements for sensing films were conducted using a source

meter (Keithley 2400). A Bruker D8 X-ray diffractometer was employed to characterize the crystallinity of the prepared CuO films. Micro-Raman spectra of the CuO film were measured using a WITec Raman Spectrometer. A field-emission scanning electron microscopy (FEI Inspect F) was used to characterize the morphology of the sensitive films.

### 3. Results and discussion

#### 3.1 Structural characterization

X-ray diffraction (XRD) result of CuO powders is shown in Fig. 2. The patterns were recorded with a Bruker D8 Advance powder X-ray diffractometer with Cu K $\alpha$  ( $\lambda = 0.15406$  nm). The powders were obtained by drying the CuO sols for 2 hours at 400 °C, and then put on glass for XRD analysis. The XRD pattern of the CuO was identified as monoclinic CuO (C2/c space group, JCPDS #48-1548). The peaks at lattice planes (110), (11-1)/(002), (111)/(200), (11-2), (20-2), (112), (020), (021), (202), (11-3), (022), (31-1)/(311), (113)/(220), (311), (004)/(22-2) are located at  $2\theta = 32.5^\circ, 35.5^\circ, 38.7^\circ, 46.2^\circ, 48.7^\circ, 51.3^\circ, 53.5^\circ, 56.7^\circ, 58.1^\circ, 61.6^\circ, 65.8^\circ, 66.4^\circ, 67.9^\circ, 72.4^\circ, 75.0^\circ$ , respectively. No other obvious peaks for impurity were found, indicating the high purity of the sensitive film. Estimated based on the Debye-Scherrer's formula, the average size of CuO particles is about 23.6 nm.

The top view and cross-section SEM images of sensitive film are shown in Fig. 3. The film is uniform and continuous with an average film thickness of 53.91 nm but with a porous surface. The average size of nanoparticles of the film is about 25 nm, which was consistent with the value estimated from XRD result.

Raman spectra of the sensitive films before and after exposure to H<sub>2</sub>S are shown in Fig. 4, in which the peaks at 292 cm<sup>-1</sup>, 339 cm<sup>-1</sup> and 626 cm<sup>-1</sup> are corresponding to A<sub>g</sub> (296 cm<sup>-1</sup>), B<sub>g</sub><sup>(1)</sup> (346 cm<sup>-1</sup>), and B<sub>g</sub><sup>(2)</sup> (636cm<sup>-1</sup>) modes of CuO crystals [27], respectively. The results in Fig. 4a, 4b and 4d demonstrate that the films before and after, exposure to 0.5 ppm H<sub>2</sub>S at RH = 30% and 50 ppm H<sub>2</sub>S at RH = 75% are all



consisted of pure CuO. In Fig. 4c, a sharp peak at  $474\text{ cm}^{-1}$  can be observed, which is assigned to the spectroscopic feature of CuS [28-32] and there are no CuO peaks observed in this spectrum, indicating that CuO has changed to CuS through the chemical reaction between  $\text{H}_2\text{S}$  and CuO when the sensitive film was exposed to 50 ppm  $\text{H}_2\text{S}$  at  $\text{RH} = 30\%$ .

### 3.2 $\text{H}_2\text{S}$ gas sensing performance

Responses of the SAW sensor to 50 ppm  $\text{H}_2\text{S}$  tested under  $\text{RH} = 30\%$  at  $25\text{ }^\circ\text{C}$  are shown in Fig. 5. The sensor exhibits a negative frequency shift, which could be attributed to the mass loading effect, elastic loading effect and electric loading effect since the temperature and pressure are kept at constant values [16]. Mass loading, elastic loading and electric effect refer to the change in mass, elasticity and resistance of the sensitive film respectively. From the previous studies [33-34], CuO can capture  $\text{H}_2\text{S}$  molecules from ambient environment (through physical adsorption), owing to extraordinary adsorptive capability of CuO to  $\text{H}_2\text{S}$  and chemical reaction between them will generate CuS on the surface of CuO particles (through chemical reaction shown in equation 1). Both the physical adsorption and chemical reaction can increase mass loading effect on the sensitive film of CuO since CuS is heavier than CuO. Chemical reaction can also lead to the change in resistance of the sensitive film. Therefore, the frequency shift may be caused by both mass loading and electric loading.



The mass loading on the film can change the central frequency ( $\Delta f$ ) of a SAW sensor as follows [35],

$$\Delta f = (\kappa_1 + \kappa_2) f_0^2 \Delta m \quad (2)$$

where  $\kappa_1 = -8.7 \times 10^{-8} \text{ m}^2\text{s kg}^{-1}$  and  $\kappa_2 = -3.9 \times 10^{-9} \text{ m}^2\text{s kg}^{-1}$  are material constants of the substrate S-T cut quartz;  $f_0 = 198.98 \text{ MHz}$  is the central frequency of SAW resonators;  $\Delta m$  is the mass loading on the SAW device. Due to the fact that both  $\kappa_1$  and  $\kappa_2$  values are negative, the increasing mass loading will cause a negative frequency shift.

The relationship between the shift of central frequency ( $\Delta f$ ) versus the surface conductivity ( $\sigma_s$ ) of the film can be described as follows [36];

$$\frac{\Delta f}{f_0} = \frac{\Delta v}{v_0} \approx -\frac{K^2}{2} \frac{\sigma_s^2}{\sigma_s^2 + v_0^2 C_s^2} \quad (3)$$

where  $C_s = 0.5 \text{ pF cm}^{-1}$ ,  $K^2 = 0.0011$ ,  $v_0 = 3158 \text{ m s}^{-1}$  and  $\sigma_s = 1/\rho$  are the surface capacitance values per unit length, the electromechanical coefficient, the undisturbed SAW velocity of quartz substrate and the sheet conductivity of the films in air, respectively. Here the central frequency of SAW resonators is  $f_0 = 198.98 \text{ MHz}$  is,  $\sigma_s = 3.0 \times 10^{-6} \text{ S m}^{-1}$  was measured by a four probe method using Keithley 2400. The acoustoelectric parameter ( $\xi = \sigma_s \cdot (v_0 C_s)^{-1}$ ) of sensitive film can be calculated and the data of frequency shift vs the acoustoelectric parameters obtained from Eq. (3) for coated SAW devices are shown in Fig. 6. The original acoustoelectric parameter (the original condition) is located at point 1, where  $\Delta f_1 / f_0 = -5.4848 \times 10^{-4}$ . After the film exposed to 50 ppm  $\text{H}_2\text{S}$ , the sheet conductivity of the film is decreased. As a result, the acoustoelectric parameter is shifted to point 2, where  $\Delta f_2 / f_0 = -5.4763 \times 10^{-4}$ .

Thus, the frequency shift caused by electric loading was calculated to be  $\Delta f = (\Delta f_2 - \Delta f_1) = -(5.4763 \times 10^{-4} - 5.4862 \times 10^{-4}) \times f_0 = -197.0$  Hz, which is much lower than the measured frequency shift. It indicates that the frequency shift was mainly contributed by the increased mass loading caused by the physical adsorption and the chemical reaction.

To further verify how these two effects contribute to the negative frequency shift under different circumstance, the sensor was tested with 0.5-50 ppm H<sub>2</sub>S with RH = 30% at 25 °C. As shown in Fig. 7a and Fig. 7b, the frequency shift was -1200 Hz when the concentration of H<sub>2</sub>S was 500 ppb and became much larger with the increase of the concentration of H<sub>2</sub>S. With the concentration of H<sub>2</sub>S up to 20 ppm, the frequency shift was ~ -15 kHz. The response and recovery times with error bars are shown in Fig. 7c. The response and recovery times are relatively shorter at lower concentrations but increased with the increase of H<sub>2</sub>S concentration. It should be noted that the sensor can't be fully recovered with the concentration of H<sub>2</sub>S, higher than 10 ppm. The increasing responses and recovery times at higher H<sub>2</sub>S concentrations indicates that the sensing mechanism of CuO to H<sub>2</sub>S with different concentrations may be different. Fig. 7d shows the response (frequency shift) over the concentration, together with error bars. The graph is not close to a linear curve. Besides, Raman spectra of the sensitive film (see Section 3.1) reveal that (1) no apparent CuS was obtained on the sensitive film after exposure to H<sub>2</sub>S at low concentrations; while (2) CuS was clearly presented at higher concentrations. Therefore, it can be concluded that; (1) reaction 1 can only happen at high

concentrations and the responses of the sensor to  $\text{H}_2\text{S}$  with low concentrations are mainly caused by physical adsorption, 2) response caused by physical adsorption is much faster than that caused by chemical reaction. Based on this analysis result, it can be proposed that it is possible to accelerate the response and recovery of the sensor by enhancing the physical adsorption and hindering the chemical reaction at the same time.

In order to prove this assumption, we have performed experiments, where the response of sensor was tested under different environments with different RH values. The reason can be explained in proceeding context; i.e. If the water is the product of reaction (1), the value of RH will have a significant impact on the sensing property of the SAW sensor. We can see that with a high RH value, chemical reaction (1) may be hindered even the concentration of  $\text{H}_2\text{S}$  is high, since there is excess  $\text{H}_2\text{O}$  on the surface of  $\text{CuO}$ .

Fig. 8 shows the experimental results, indicating the response becomes obviously stronger and faster with the increase of the RH. Moreover, Raman spectrum analysis was also performed and the results revealed that no  $\text{CuS}$  was produced on the sensitive film at a high RH level, even if the film was exposed to 50 ppm  $\text{H}_2\text{S}$ , based on these results, it can be concluded that; (1) reaction 1 was hindered at higher RH value; and (2) physical adsorption was enhanced at a higher RH value. From literature, the adsorption capacity of  $\text{CuO}$  to  $\text{H}_2\text{S}$  is stronger than that of  $\text{CuS}$  [24, 37-39]. Besides, the  $\text{CuS}$  on the surface of the  $\text{CuO}$  particles will act as a barrier and reduce the direct contact between  $\text{H}_2\text{S}$  gas and  $\text{CuO}$  particles. With less  $\text{CuS}$  on the film (less

chance of chemical reaction occurrence), more CuO particles are able to contact the H<sub>2</sub>S gas and the adsorption capacity of the CuO film to H<sub>2</sub>S is stronger.

The SAW sensor was tested with 0.5 ppm-10 ppm H<sub>2</sub>S with RH= 75 % at 25 °C and the result was shown in Fig. 9a. The response and recovery time are gradually increased with the increase of H<sub>2</sub>S concentration. Compared with the response values obtained at RH = 30%, those at 75% RH are much stronger, the response and recovery times at RH = 75% are much shorter. Fig. 9c shows the response (frequency shift) over the concentration, together with error bars. The image is very close to a linear curve. These results confirm further, the influence of RH on the response. As a result, the SAW sensor based on CuO has a stronger and faster response to H<sub>2</sub>S at a high RH, indicating that this sensor is promising for the application of detection of H<sub>2</sub>S at a high RH.

The selectivity of the sensor was also investigated by exposing the sensor in the chamber with RH = 75% at 25 °C and then injected with 50 ppm of H<sub>2</sub>, C<sub>2</sub>H<sub>5</sub>OH, acetone, NH<sub>3</sub>, CO, NO, NO<sub>2</sub> and ethyl-mercaptan and 10 ppm of H<sub>2</sub>S successively into the chamber. The whole results are shown in Fig. 10a and its magnification is shown in Fig. 10b. It is obvious that the response to H<sub>2</sub>, C<sub>2</sub>H<sub>5</sub>OH, acetone, NH<sub>3</sub>, CO, NO, NO<sub>2</sub> and ethyl-mercaptan are much weaker compared to that of H<sub>2</sub>S, signifying its excellent selectivity. This excellent selectivity is attributed to the extraordinary adsorptive capability of CuO to H<sub>2</sub>S.

The stability of the SAW sensor was tested with exposure to 2 ppm H<sub>2</sub>S in the environment with 75% RH for 4 successive cycles. As shown in Fig. 11, the sensor

shows similar responses in four successive cycles, demonstrating that the sensors have a good stability. The response time and recovery time are slightly different, which is attributed to the operating error. In order to see the shifts of base lines and magnitudes, we did 15 consecutive experiments of 2 ppm and 10 ppm at RH=75%. The results are shown in Fig.12. The fluctuations of base line are smaller than 300 Hz. The fluctuation of frequency shift is less than 5% for the fifteen consecutive tests, indicating good reproducibility.

### 3. Conclusions

In this work, we investigated a SAW H<sub>2</sub>S gas sensor based on porous CuO films, prepared using sol–gel method at room temperature. The CuO films have a porous surface composed of a lot of nanoparticles having an average size of about 25 nm. The SAW sensor showed negative frequency shifts toward H<sub>2</sub>S gas, caused by the increase of mass loading. The SAW sensor exhibited better sensing performance in the environment with a higher RH, since the chemical reaction between H<sub>2</sub>S and CuO is hindered. The sensor showed a good selectivity towards H<sub>2</sub>S at higher RH values at room temperature.

### Acknowledgments

The authors acknowledge the support by the National Natural Science Foundation of China U1630126, Funding supports from UK Engineering Physics and Science Research Council (EPSRC EP/P018998/1), Newton Mobility Grant (IE161019) through Royal Society and NFSC, and Royal academy of Engineering UK-Research Exchange with China and India are also acknowledged. And this work is also supported by the Fundamental Research Funds for the Central Universities (No.A0920502051904-67)

**Reference:**

- [1] C. Chairunissa, T. Arslan, *Ieee*, Design of a Dual-Function Antenna for Microwave Gas Detection and Communication in Industrial Wireless Sensor Network Applications, New York: *Ieee*; 2017.
- [2] C. Di Natale, A. Macagnano, E. Martinelli, R. Paolesse, G. D'Arcangelo, C. Roscioni, et al., Lung cancer identification by the analysis of breath by means of an array of non-selective gas sensors, *Biosens. Bioelectron.*, 18(2003) 1209-18.
- [3] D.W. Dockery, J. Schwartz, J.D. Spengler, air- pollution and daily mortality-associations with particulates and acid aerosols, *Environ. Res.*, 59(1992) 362-73.
- [4] N. Docquier, S. Candel, Combustion control and sensors: a review, *Rrog. Energ. Combust.*, 28(2002) 107-50.
- [5] D. Kohl, Function and applications of gas sensors, *J. Phys. D-Appl. Phys.*, 34(2001) R125-R49.
- [6] E. Baraldi, S. Carra, C. Dario, N. Azzolin, R. Ongaro, G. Marcer, et al., Effect of natural grass pollen exposure on exhaled nitric oxide in asthmatic children, *A.m. J. Respir. Crit. Care. Med.*, 159(1999) 262-6.
- [7] M.N. Bates, J. Crane, J.R. Balmes, N. Garrett, Investigation of Hydrogen Sulfide Exposure and Lung Function, Asthma and Chronic Obstructive Pulmonary Disease in a Geothermal Area of New Zealand, *PLoS One*, 10(2015) 16.



- [8] W.J. Gauderman, E. Avol, F. Lurmann, N. Kuenzli, F. Gilliland, J. Peters, et al., Childhood asthma and exposure to traffic and nitrogen dioxide, *Epidemiology*, 16(2005) 737-43.
- [9] L. Preller, D. Heederik, J.S.M. Boleij, P.F.J. Vogelzang, M.J.M. Tielen, Lung -function and chronic respiratory symptoms of pig farmers-focus on exposure to endotoxins and ammonia and use of disinfectants, *Occup. Environ. Med.*, 52(1995) 654-60.
- [10] M.T. Salam, J. Millstein, Y.F. Li, F.W. Lurmann, H.G. Margolis, F.D. Gilliland, Birth outcomes and prenatal exposure to ozone, carbon monoxide, and particulate matter: Results from the children's health study, *Environ. Health Perspect.*, 113(2005) 1638-44.
- [11] K. Eto, T. Asada, K. Arima, T. Makifuchi, H. Kimura, Brain hydrogen sulfide is severely decreased in Alzheimer's disease, *Biochem. Biophys. Res. Commun.*, 293(2002) 1485-8.
- [12] O. Kabil, R. Banerjee, Redox Biochemistry of Hydrogen Sulfide, *J. Biol. Chem.*, 285(2010) 21903-7.
- [13] A. Pohl, A review of wireless SAW sensors, *IEEE T. Ultrason. Ferr.*, 47(2000) 317-32.
- [14] L. Rana, R. Gupta, M. Tomar, V. Gupta, ZnO/ST-Quartz SAW resonator: An efficient NO<sub>2</sub> gas sensor, *Sens. Actuators, B*, 252 (2017): 840-845.

- [15] W. Wen, S.T. He, S.Z. Li, M.H. Liu, P. Yong, Enhanced sensitivity of SAW gas sensor coated molecularly imprinted polymer incorporating high frequency stability oscillator, *Sens. Actuators, B*, 125(2007) 422-7.
- [16] Y.L. Tang, Z.J. Li, J.Y. Ma, H.Q. Su, Y.J. Guo, L. Wang, et al., Highly sensitive room-temperature surface acoustic wave (SAW) ammonia sensors based on  $\text{Co}_3\text{O}_4/\text{SiO}_2$  composite films, *J. Hazard. Mater.*, 280(2014) 127-33.
- [17] N.S. Ramgir, S. Kailasa Ganapathi, M. Kaur, N. Datta, K.P. Muthe, D.K. Aswal, S.K. Gupta, J.V. Yakhmi, Sub-ppm  $\text{H}_2\text{S}$  sensing at room temperature using CuO thin films, *Sens. Actuators, B*, 151 (2010) 90–96.
- [18] H.J. Kim, J.H. Lee, Highly sensitive and selective gas sensors using p-type oxide semiconductors: Overview, *Sens. Actuators, B*, 192(2014) 607-27.
- [19] S.J. Patil, A.V. Patil, C.G. Dighavkar, K.S. Thakare, R.Y. Borase, S.J. Nandre, et al., Semiconductor metal oxide compounds based gas sensors: A literature review, *Front. Mater. Sci.*, 9(2015) 14-37.
- [20] S. Sonia, P.S. Kumar, N.D. Javram, Y. Masuda, D. Mangalaraj, C.M. Lee, Superhydrophobic and  $\text{H}_2\text{S}$  gas sensing properties of CuO nanostructured thin films through a successive ionic layered adsorption reaction process, *RSC Adv.* 6 (2016) 24290–24298.
- [21] X.B. Hu, Z.G. Zhu, C. Chen, T.Y. Wen, X.L. Zhao, L.L. Xie, Highly sensitive  $\text{H}_2\text{S}$  gas sensors based on Pd-doped CuO nanoflowers with low operating temperature, *Sens. Actuators, B*, 253(2017) 809-17.

- [22] N. Haimour, R. El-Bishtawi, A. Ail-Wahbi, Equilibrium adsorption of hydrogen sulfide onto CuO and ZnO, *Desalination*, 181(2005) 145-52.
- [23] J.A. Rodriguez, A. Maiti, Adsorption and decomposition of H<sub>2</sub>S on MgO(100), NiMgO(100), and ZnO(0001) surfaces: A first-principles density functional study, *J. Phys. Chem. B*, 104(2000) 3630-8.
- [24] M. Xue, R. Chitrakar, K. Sakane, K. Ooi, Screening of adsorbents for removal of H<sub>2</sub>S at room temperature, *Green Chem.*, 5(2003) 529-34.
- [25] J. Chen, K. Wang, L. Hartman, W. Zhou, H<sub>2</sub>S detection by vertically aligned CuO nanowire array sensors. *J. phys. chem. C*, 112(2008), 16017-16021.
- [26] Y.L. Tang, Z.J. Li, J.Y. Ma, L. Wang, J. Yang, B. Du, et al., Highly sensitive surface acoustic wave (SAW) humidity sensors based on sol-gel SiO<sub>2</sub> films: Investigations on the sensing property and mechanism, *Sens. Actuators, B*, 215(2015) 283-91.
- [27] X.K. Chen, J.C. Irwin, J.P. Franck, Evidence for a strong spin-phonon interaction in cupric oxide, *Phys. Rev. B*, 52(1995) R13130.
- [28] B. Minceva-Sukarova, M. Najdoski, I. Grozdanov, C. J. Chunnillall, Raman spectra of thin solid films of some metal sulfides, *J. Mol. Struct.* 1997, 267, 410.
- [29] M. Bouchard, D. C. Smith, Catalogue of 45 reference Raman spectra of minerals concerning research in art history or archaeology, especially on corroded metals and coloured glass, *Spectrochim. Acta. A*, 2003, 59, 2247.
- [30] K. Xu, W. Ding, Controlled synthesis of spherical CuS hierarchical structures, *Mater. Lett.*, 2008, 62, 4437.

- [31] S.Y. Wang, W. Wang, Z.H. Lu, Asynchronous-pulse ultrasonic spray pyrolysis deposition of  $\text{Cu}_x\text{S}$  ( $x= 1, 2$ ) thin films, *Mater. Sci. Eng. B-Solid*, 2003, 103, 184.
- [32] G. D. Smith, R. J. H. Clark, The role of  $\text{H}_2\text{S}$  in pigment blackening, *J. Cult. Herit.*, 2002, 3, 101.
- [33] H. Kim, C. Jin, S. Park, S. Kim, C.M. Lee,  $\text{H}_2\text{S}$  gas sensing properties of bare and Pd-functionalized CuO nanorods, *Sens. Actuators, B*, 161 (2012) 594–599.
- [34] X.P. Li, Y. Wang, Y. Lei and Z.y. Gu, Highly sensitive  $\text{H}_2\text{S}$  sensor based on template-synthesized CuO nanowires. *Rsc Adv.*, 2012, 2(6): 2302-2307.
- [35] D.S. Ballantine Jr., S.J. Martin, A.J. Ricco, G.C. Frye, H. Wohltjen, R.M. White, E.T.Zellers, Acoustic Wave Sensors: Theory, Design, and Physico-Chemical Applications, *Academic Press*, San Diego, 1997.
- [36] A.J. Ricco, S.J. Martin, T.E. Zipperian, Surface acoustic wave gas sensor based on film conductivity changes, *Sens. Actuators, B*, 8 (1985) 319–333.
- [37] R.B. Vasiliev, M.N. Rumyantseva, N.V. Yakovlev, A.M. Gaskov, CuO/SnO<sub>2</sub> thin film heterostructures as chemical sensors to  $\text{H}_2\text{S}$ , *Sens. Actuators, B*, 50(1998) 186-93.
- [38] A. Galtayries, J.P. Bonnelle, XPS and ISS studies on the interaction of  $\text{H}_2\text{S}$  with polycrystalline Cu, Cu<sub>2</sub>O and CuO surfaces, *Surf. Interface Anal.*, 23(1995) 171-9.
- [39] T. Chivers, J. B. Hyne, and C. Lau., The thermal decomposition of hydrogen sulfide over transition metal sulfides, *Int. J. Hydrogen. Energ.*, 5 (1980): 499-506.

**Figure caption**

Fig. 1. (a) Schematic diagram of a SAW sensor; (b) Top view of the SAW sensor sample.

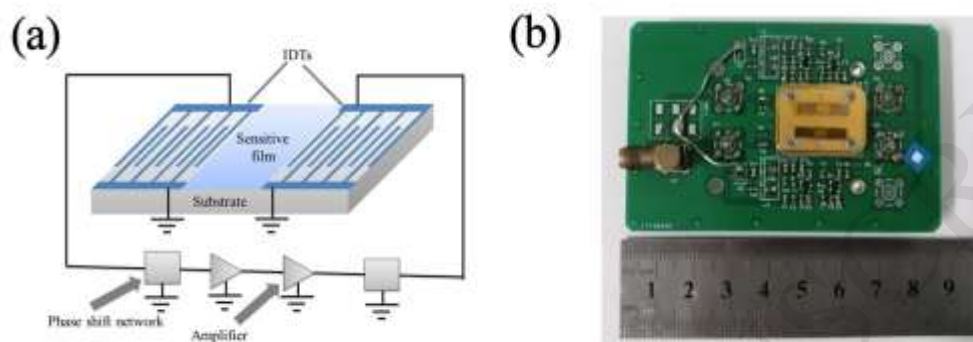


Fig. 2. XRD patterns of as-prepared CuO powders.

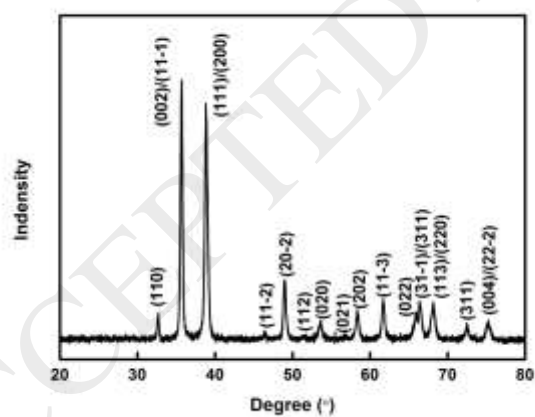


Fig. 3. SEM image of top-view and cross-section view of as-synthesized CuO film.

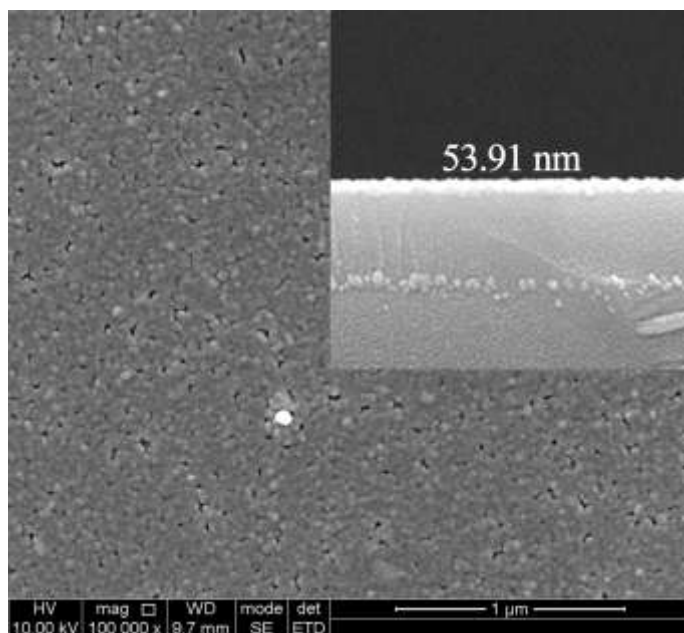


Fig. 4. Raman spectra of CuO sensitive film: (a) the original CuO film; (b) film surface exposed to 0.5 ppm H<sub>2</sub>S at RH = 30%; (c) film surface exposed to 50 ppm H<sub>2</sub>S at RH = 30%; (d) film surface exposed to 50 ppm H<sub>2</sub>S at RH = 75%.

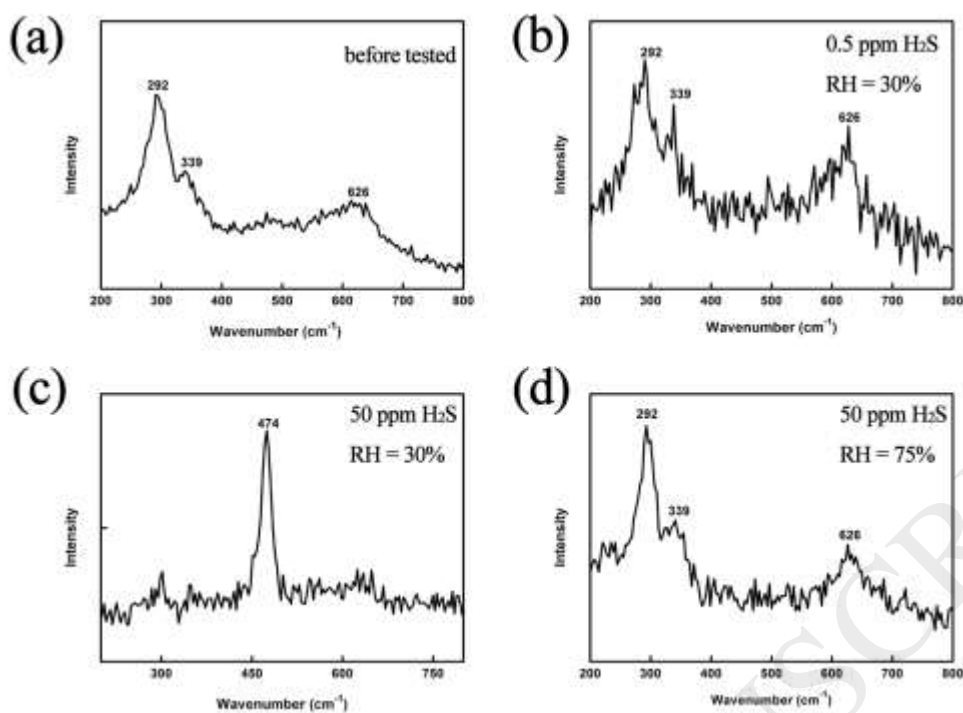


Fig. 5. Responses of the SAW sensor to 50 ppm H<sub>2</sub>S with RH = 30% at 25 °C.

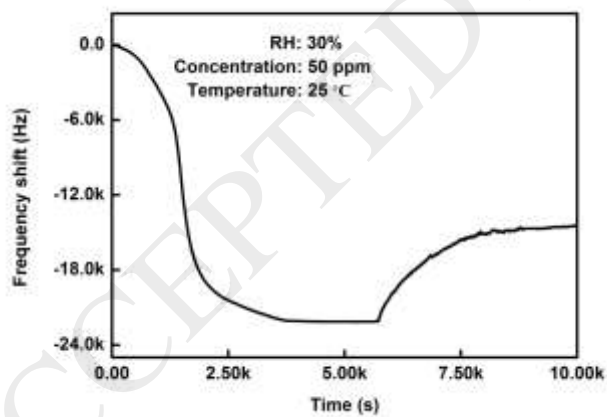


Fig. 6. Plot of frequency changes versus acoustoelectric parameter ( $\xi = \sigma_s \cdot (v_0 C_s)^{-1}$ ).

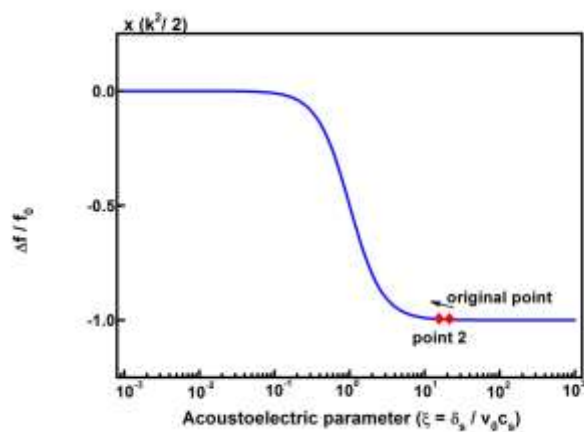


Fig. 7. (a) Dynamic responses of the sensor to 0.5-10 ppm H<sub>2</sub>S with RH = 30% at 25 °C; (b) The responses of the sensor to 20 ppm and 50 ppm H<sub>2</sub>S; (c) the response and recovery time versus the H<sub>2</sub>S concentration.

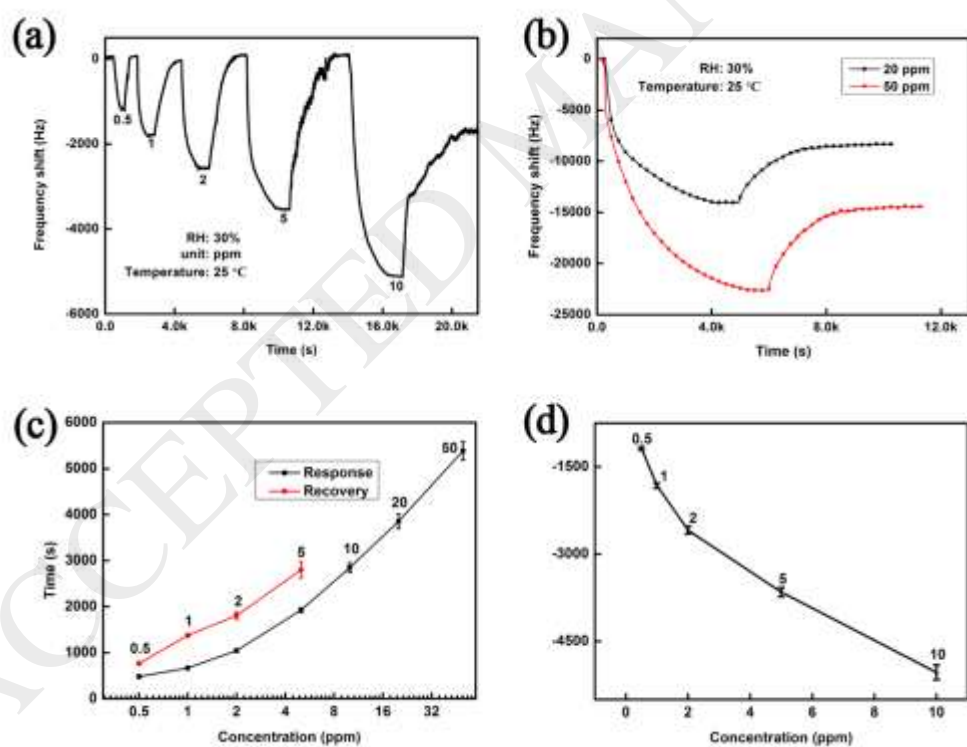


Fig. 8. (a) Dynamic response of the sensor to 10 ppm H<sub>2</sub>S with various RH at 25 °C; (b) the response and recovery time versus the RH.



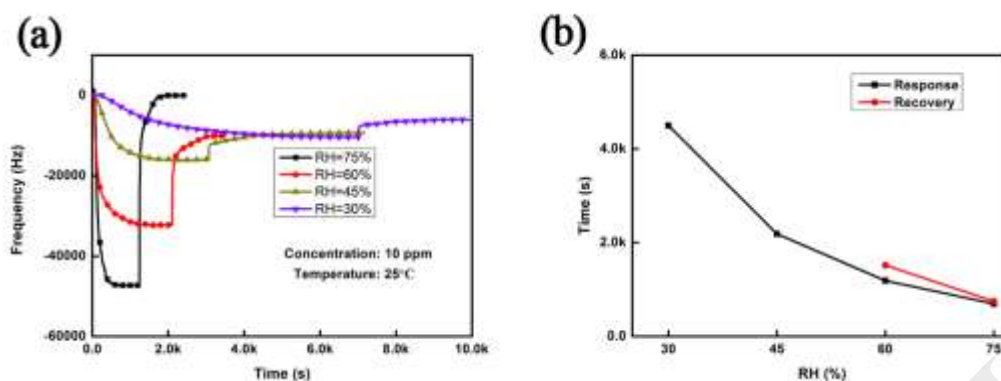


Fig.9. (a) Dynamic response of the sensor to H<sub>2</sub>S of various concentrations with RH = 75% at 25 °C; (b) the response and recovery time versus the concentration.

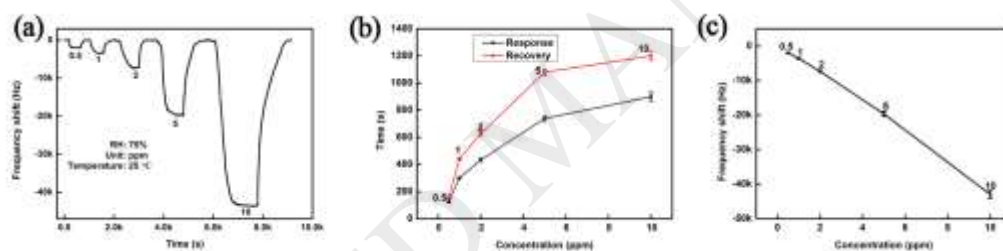


Fig. 10. (a) Response under different gas with RH=75% at 25 °C; (b) the magnification of (a).

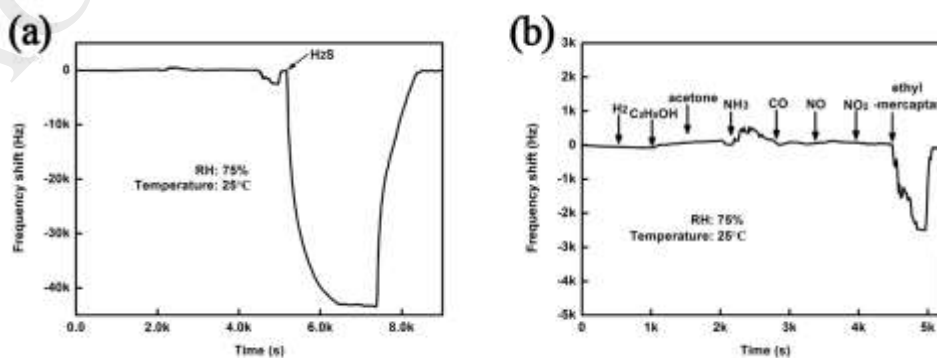


Fig. 11. Short term stability testing by exposing the sensors to 2 ppm H<sub>2</sub>S with RH=75% at 25 °C for a few cycles.

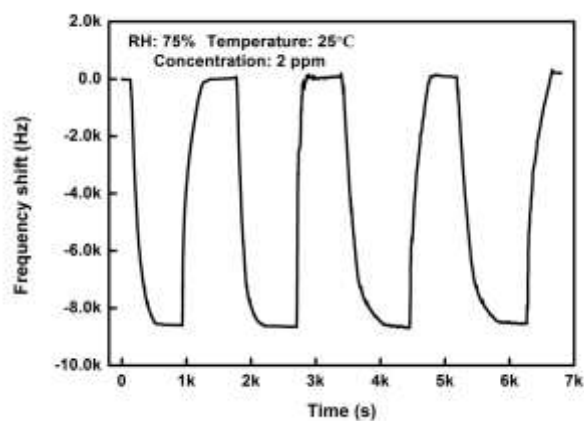
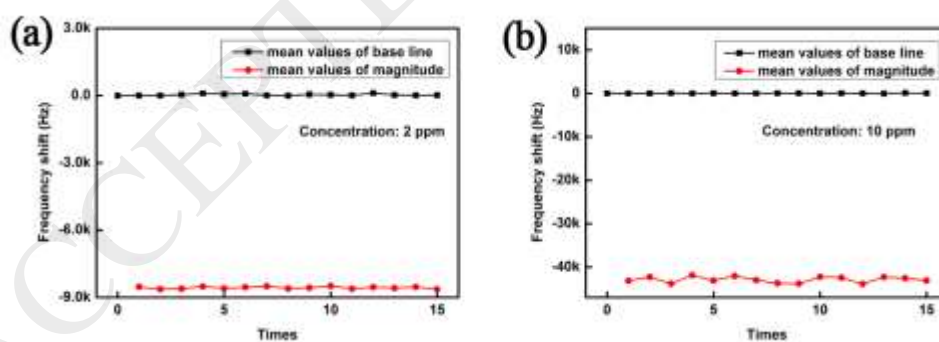


Fig. 12. The frequency shifts of base line and magnitude in 15 consecutive experiments of (a) 2 ppm and (b) 10 ppm at RH=75%



**Author Biographies**

**Deng-Ji Li** obtained his B.S. degree in School of Physic, Wuhan University. He is a postgraduate student in Institute of Fundamental and Frontier Sciences at University of Electronic Science and Technology of China. His current research interests focus on sensing devices using acoustic wave technology applications of nanomaterials and novel functional materials.

**Yong-Liang Tang** obtained his PH.D. degree from University of Electronic Science and Technology of China in 2017. He is now an associate Professor in School of Physical Science and Technology at Southwest Jiaotong University. His present interests include applications of nanomaterials and functional thin films for sensors and surface acoustic wave (SAW) devices.

**Dong-yi Ao** obtained his B.S. degree in School of Management and Economics, University of Electronic Science and Technology of China in 2012. He is a Ph.D. student in School of Physical Electronics at University of Electronic Science and Technology of China. His present interests include applications of nanomaterials and functional thin films for sensors and surface acoustic wave (SAW) devices, graphene preparation and applications.

**Qing-Bo Tang** obtained his B.S. degree in School of Computer and Information, China Three Gorges University in 2016. He is a Master Degree Candidate in School

of Physical at University of Electronic Science and Technology of China. His current research interests focus on sensing devices using acoustic wave technology, microfluidics and interaction between laser and solid material.

**Richard Yong-Qing Fu** received his Ph.D. degree from Nanyang Technological University, Singapore in 1999, and now worked in Mathematics Physics and Electrical Engineering, Northumbria University, UK. His recent research has been focusing on piezoelectric and shape memory films, nanostructured composite/films for applications in MEMS, sensing and energy applications.

**Yuan-Jun Guo** received his Ph.D. from Shanghai Institute of Optics and Fine Mechanics, Chinese Academy of Sciences in 2006. From July 2011, he became an associate Professor in School of Physical, University of Electronic Science and Technology of China. His current research interests focus on sensing devices using acoustic wave technology, microfluidics and interaction between laser and solid material.

**Bilawal Khan** obtained his B.S. degree in Shah Abdul Latif University Khairpur, Sindh, Pakistan. Now he is a Master Degree Candidate in School of Physical at University of Electronic Science and Technology of China. His current research interests focus on preparation and application of Nanomaterials.

**M.Bilal Faheem** is a Ph.D. student in School of Physical Electronics at University of Electronic Science and Technology of China. His research interests include Pollutants degradation, Solar water oxidation, Water splitting, Material Science, Nano Science

**Xiao-Tao Zu** received his Ph.D. degree from Sichuan University in 2002. He is a Professor in Institute of Fundamental and Frontier Sciences at University of Electronic Science and Technology of China. His research interests include photoelectric materials, smart materials, composite nanomaterials and their industrial applications.

**Li Li** is now a vice Professor in School of Physics at University of Electronic Science and Technology of China. Her research interests include advanced functional materials, thermal analysis, computational materials, thin film and nanotechnology

**Sean Li** is now a Professor in School of Materials Science & Engineering at the University of New South Wales in Sydney. His research interests include advanced electronic and photonic materials, energy and thermoelectric materials, thermal analysis, advanced materials characterization, computational materials, thin film and nanotechnology